

GEANT4 Study of Proton–Body Interactions

J.A. López^{1*}, S.S. Romero González¹, O. Hernández Rodríguez¹, J. Holmes² and R. Alarcon²

¹Physics Department, University of Texas at El Paso, El Paso, Texas, 79968 USA

²Physics Department, Arizona State University, Tempe, Arizona, 85281 USA

*jorgelopez@utep.edu (Corresponding Author)

ARTICLE INFORMATION

Received: September 18, 2020
Accepted: January 09, 2021
Published Online: February 10, 2021

Keywords:

Proton therapy, Gamma rays, GEANT4



DOI: 10.15415/jnp.2021.82015

ABSTRACT

Proton therapy uses a beam of protons to destroy cancer cells. A problem of the method is the determination of what part of the body the protons are hitting during the irradiation. In a previous study we determine that by capturing the gamma rays produced during the irradiation one can determine the location of the proton-body interaction, in this work we investigate if by examining the gamma rays produced it is possible to determine the body part that produced the gamma rays by the proton collision. This study uses GEANT4 computer simulations of interactions of proton-tissue, proton-brain, proton-bone, etc., which produce gamma rays, to determine the characteristics of the gamma rays produced. We then analyze the characteristics of the gamma rays to find signatures that could be used to determine the source of the rays. In particular, we study the distribution of gamma ray energies, their full-width half-maximum, energy resolution, maximum height, and total number of counts. This study concludes that it is possible to use the gamma ray spectra to determine what body part produced it.

1. Introduction

Proton therapy uses a beam of protons to irradiate diseased tissue. An advantage of proton therapy over other types of treatments is the ability of the protons to deposit energy in a narrow range minimizing irradiation to healthy cells.

Calibrating the proton energy allows to deposit energy in a certain range known as the Bragg peak [1]. Figure 1 (A) shows a typical spread-out Bragg peak (SOBP) of a proton beam produced by twelve Bragg peaks (blue lines) at different energies [2], compared to the X-ray range. Typically, proton beams have energies in the range of 70 to 250 MeV [4].

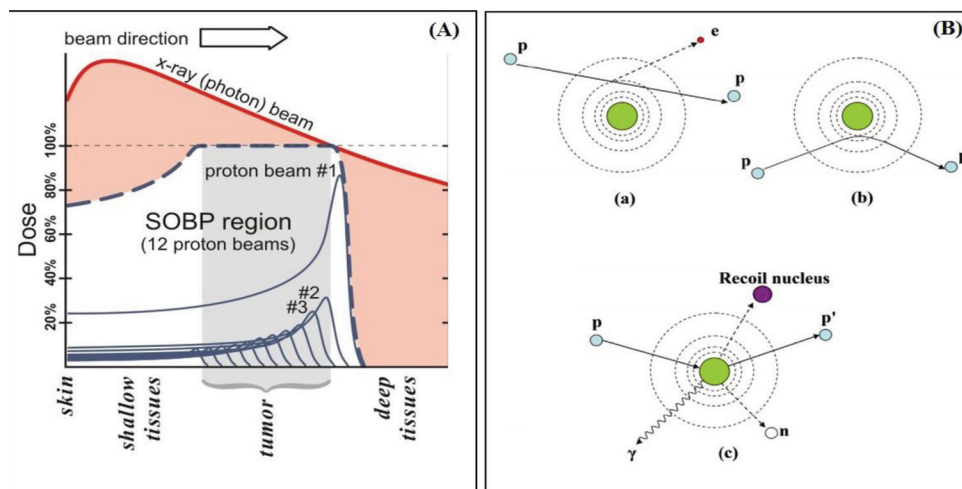


Figure 1: (A) Spread of x-ray radiation compared to proton radiation. The spread-out Bragg peak (SOBP) is actually produced by several Bragg peaks (blue lines) at different energies [2]. (B) Proton interaction mechanisms: (a) proton-electron interactions, (b) deflection of proton by the nucleus Coulomb field, (c) proton-nucleus collision [3].

parts) and produce gamma rays, which are allowed to travel unperturbed. Outside the medium, the energy and direction of the gamma rays is analyzed through CERN's interface ROOT. The simulations include a "world", a proton beam, and a "water phantom" representing both the target and the counter. The simulations were performed with different target materials composed of different body compounds (tissue, blood, bone, brain, etc.), created with GEANT4's material database [10]. Proton energies used were 60 MeV, 80 MeV and 120 MeV. The simulations were computed in a personal computer with Intel i7 processors and each run lasted up to 20 minutes. Altogether close to one billion runs were simulated. Figure 3 shows the world (large external cube), protons (blue lines) hitting the water phantom (inside cube), producing gamma rays (green lines) and electrons (red lines).

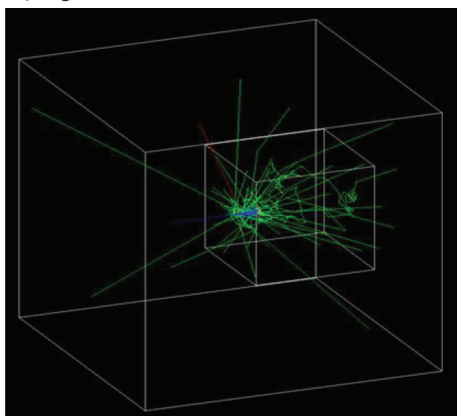


Figure 3: GEANT4 Simulation of protons hitting a cube of water.

4. Results

The energy spectra were obtained with ROOT, further analysis includes a Gaussian fit of the resonant peaks, the areas under the peaks, the full width half maximum (FWHM), the maximum number of counts, and the peak resolution. The media studied were water, MS20 tissue, lung, brain, bone, blood, tissue, muscle with sucrose and without sucrose, muscle striated ICRU, and muscle skeletal ICRP. Histograms contain 10,000,000 events of proton colliding with the targets. Figure 4 shows typical spectra obtained for water, MS20 Tissue, brain and bone.

Next, the observed spectra were compared on a peak-by-peak basis. For this, the seven most prominent peaks of the water spectrum (2.0 MeV, 2.31 MeV, 2.8 MeV, 3.68 MeV, 4.44 MeV, 5.2 MeV, 6.1 MeV) were characterized by

fitting them with a Gaussian curve:
$$Y = \frac{1}{\sqrt{2\pi\sigma^2}} e^{-\frac{(E-E_0)^2}{2\sigma^2}}$$
, where Y is the gamma count, E_0 is the mean energy of the peak, and σ is the standard deviation, all obtained with the software package Origin. Furthermore, the energy resolution (R) of each peak is the FWHM expressed as a percentage of the mean energy, $R = FWHM \times 100/E_0$; R is important for the design of the detector, scintillation counting equipment in nuclear medicine typically have resolutions of less than 10%. Figure 5 shows the comparison of water and tissue peaks and Gaussian fits, Table 2 shows the number of gamma rays produced in each of the seven peaks of the nine target materials at the selected energies, and compared to water in percentages.

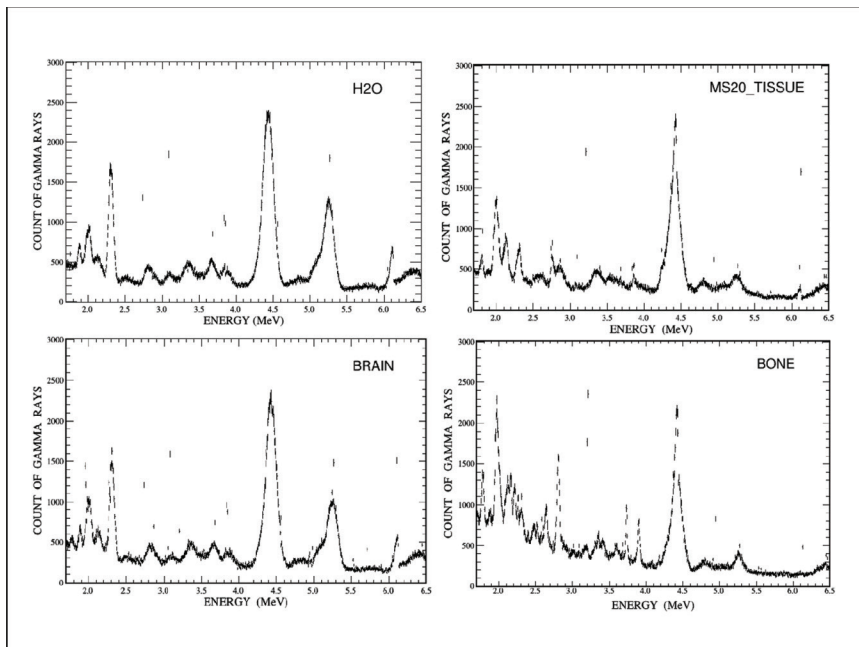


Figure 4: Gamma ray spectra of water, MS20 Tissue, brain and bone.

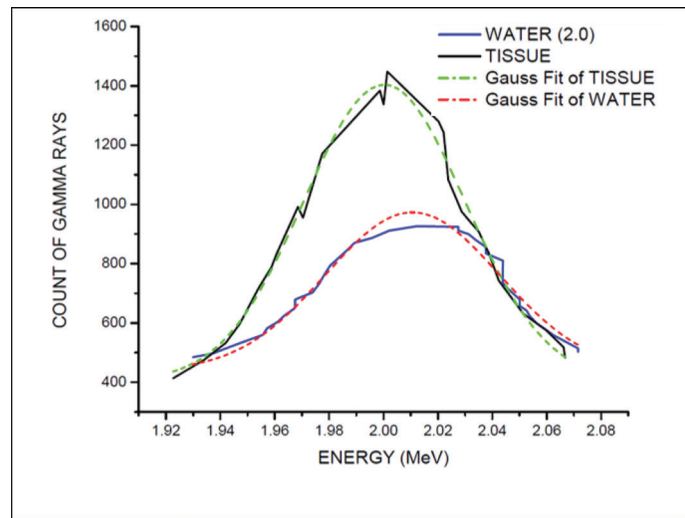


Figure 5: Example of comparison of water and tissue peaks and Gaussian fits.

Table 2. Integration peaks of body materials normalized respect to water.

MATERIAL	2.00 MeV	2.31 MeV	2.80 MeV	3.68 MeV	4.44 MeV	5.20 MeV	6.10 MeV
WATER	7572	12759	10500	7604	16463	8598	10177
WATER NORMALIZED (N)	100%	100%	100%	100%	100%	100%	100%
TISSUE	8483	12444	6568	6613	8822	8113	5438
TISSUE N	112.03%	97%	62.55%	86.97%	53.59%	94.3%	53.43
BONE	20189	24968	12523	9314	19004	9906	7623
BONE N	266.63%	195.69%	119.27%	122.49%	115.43%	115.21%	74.90%
BLOOD	8132	13517	10503	7781	15812	8790	9707
BLOOD N	107.40%	105.94%	100.03%	102.33%	96.05%	102.23%	95.38%
BRAIN	8399	13431	10173	7737	15412	8670	9410
BRAIN N	110.92%	105.27%	96.8%	101.75%	93.62%	100.84%	92.46%
LUNG	8338	13299	10646	7757	15977	8806	9797
LUNG N	110.12%	104.23%	101.39%	102.01%	97.05%	102.42%	96.27%
MS20 TISSUE	11486	16675	9168	7967	13396	11478	9157
MS20 TISSUE N	151.69%	130.69%	87.31%	104.77%	81.37%	133.50%	89.98%
MUSCLE STRIATED ICRU	8072	12990	10081	7643	15216	8693	9507
MUSCLE STRIATED ICRU N	106.60%	101.81%	96.01%	100.51%	92.43%	101.1%	93.42%
MUSCLE WITHOUT SUCROSE	7606	12649	9997	7650	15359	8525	9379
MUSCLE WITHOUT SUCROSE N	100.45	99.14%	95.21%	100.60%	93.29%	99.15%	92.16%

In summary, we present some of the most interesting features observed in the hundreds of peaks studied.

- For the peak at 3.68 MeV the lung's area is less than water's by 30%, and for the peak at 2.3 MeV the difference is around 15%. These two points are promising signatures to distinguish between lung and water.
- For the peak at 3.68 MeV the tissue's FWHM is bigger than water's by more than 300%, and for the 5.2 MeV peak is around 400% greater.

- There is a pronounced difference in the values of Max Height for blood, water, or tissue and, thus, it is possible to distinguish between these materials at some energies.
- Tissue differs in area by 30% with respect to water or lung at the 2 MeV peak, by 75% at the 2.3 MeV peak, and by about 150% at the 3.68 MeV peak.
- Water, tissue and MS20-tissue have similar spectra, but at the energy of 3.68 MeV muscle (of any kind) yields less gammas than water.

- R for water, tissue and MS20-tissue present major differences at 3.68 MeV, where R for MS20-tissue it is greater by 100% than water. This is due to the fact that tissue nor MS20-Tissue does not present a peak at such energy.
- At 2 MeV, MS20-tissue and normal tissue differ from water by about 50% at the same energies. The comparisons of the seven peaks of some of the targets are presented in Table 3; results labelled as NA (Not Applicable) indicate that the Gaussian fit was not accurate.

Table 3: Peak comparison of water and body materials.

	Xc(ENERGIES KeV)	FWHM(KeV)	R%	MAX HIGH	INTEGRATION OF PEAKS
WATER	2000	75.3	3.76	973.21	78009.44
	2310	74.98	3.24	1784.6	142440.00
	2800	160.42	5.72	453.01	77359.19
	3680	118.11	3.20	541.94	68137.08
	4440	165.65	3.73	2394.25	422188.69
	5200	153.0.8	2.94	1249.27	203573.11
	6200	63.89	1.03	638.29	43410.68
TISSUE	2000	69.92	3.49	1403.39	104454.09
	2310	78.2	3.38	482.41	40157.68
	2800	NA	NA	510	NA
	3680	NA	NA	331.46	NA
	4440	109.65	2.46	1843.41	215167.28
	5200	NA	NA	199.06	NA
	6200	24.37	0.39	152.57	3957.95
LUNG	2000	77.33	3.86	984.83	81069.02
	2310	69.22	2.99	1604.75	118245.50
	2800	NA	NA	456.83	NA
	3680	84.01	2.28	520.12	46513.62
	4440	166.43	3.74	2290.39	405776.33
	5200	158.35	3.04	1109.59	187036.45
	6200	63.42	1.02	587.55	39665.84
BRAIN	2000	69.13	3.45	1013.94	74614.71
	2310	71.13	3.07	1478.34	111936.77
	2800	130.23	4.65	461.76	64013.71
	3680	84.55	2.29	483.38	43505.87
	4440	162.24	3.65	2240.09	386873.57
	5200	157.6	3.03	1004.05	168444.64
	6200	71.22	1.14	533.56	40451.15
BONE	2000	50.85	2.54	2133.85	115504.92
	2310	55.19	2.39	1203.1	70681.83
	2800	42.87	1.53	1544.02	70461.53
	3680	15.98	0.43	981.73	16699.92
	4440	110.92	2.49	1846.09	217975.85
	5200	113.08	2.17	384.52	46286.08
	6200	34.78	0.56	169.11	6261.01

BLOOD	2000	73.6	3.68	1030.22	80714.85
	2310	70.36	3.04	1600.25	119855.87
	2800	138.55	4.94	455.79	67222.86
	3680	78.78	2.14	509.82	42754.17
	4440	165.59	3.72	2252.65	397075.86
	5200	157	3.02	1075.85	179803.04
	6200	57.24	0.92	548.33	33410.83

Conclusions

The goal of this study was to determine the type of target being irradiated by inspecting the gamma rays produced in proton therapy. We performed GEANT4 simulations of proton-body interactions and studied the gamma rays produced in such interactions. The analysis was performed for 10 body materials, namely, MS20 tissue, lung, brain, bone, blood, tissue, muscle with sucrose and without sucrose, muscle striated ICRU, and muscle skeletal ICRP. The gamma ray peaks studied were those at the energies of the seven main gamma peaks produced in proton-water collisions, at energies 2.0, 2.3, 2.8, 3.68, 4.44, 5.2, and 6.1 MeV. Characterizing such peaks, a comparison between the peaks produced by different body parts was performed.

Part of the results are shown in Table 3, and they show that indeed it is possible to use the gamma rays emitted at certain energies to identify the target that produced the rays by proton collision. Although this study is a good start, there are limitations related to the sensibility of the gamma ray detectors to be used, and further studies are necessary.

Innovations and Contributions

The main innovation and contribution of this article is to introduce a way to identify the target (body part) being hit by the proton beam in proton therapy.

Acknowledgements

J.A.L. acknowledges support from UTEP's BUILDING SCHOLARS Program. This work was part of the M.S. thesis of O. Hernández Rodríguez [11].

References

- [1] K.A. Camphausen and R.C. Lawrence, Cancer Management: A Multidisciplinary Approach. In: *Principles of Radiation Therapy*, edited by R. Pazdur, L.D. Wagman, K.A. Camphausen and W.J. Hoskins, 11th ed., Cmp. United Business Media, 2009.
- [2] W.P. Levin, H. Kooy, J.S. Loeffler and T.F. DeLaney, *British Journal of Cancer* **93**, 849 (2005).
<https://doi.org/10.1038/sj.bjc.6602754>
- [3] W.D. Newhauser and R. Zhang, *Phys. Med. Biol.* **60**, R155 (2015).
<https://doi.org/10.1088/0031-9155/60/8/R155>
- [4] J. Metz, Differences between protons and X-rays. Abramson Cancer Center of the University of Pennsylvania, 2006. Retrieved on February 04, 2018 from <http://www.oncolink.org/treatment/article.cfm?c=9&s=70&id=210>.
- [5] J.A. López, S.S. Romero González, O. Hernández Rodríguez, J. Holmes and R. Alarcón, *Journal of Nuclear Physics Material Sciences Radiation and Applications* **7**, 217 (2020).
<https://doi.org/10.15415/jnp.2020.72028>
- [6] S.S. Romero Gonzalez, M.S. Thesis, University of Texas at El Paso, 2018. Retrieved on September 14, 2020 from <https://scholarworks.utep.edu/dissertations/AAI10822888/>.
- [7] R. Alarcon, D. Blyth, E. Galyaev, J. Holmes, L. Ice, G. Randall, M. Bues and M. Fatyga, *Int. J. Modern Physics: Conference Series* **44**, 1660217 (2016).
<https://doi.org/10.1142/S2010194516602179>.
- [8] Basics physics of nuclear medicine/interaction of radiation with matter. Retrieved on September 14, 2020 from https://en.wikibooks.org/wiki/Basic_Physics_of_Nuclear_Medicine/Interaction_of_Radiation_with_Matter.
- [9] Geant4 Collaboration. Introduction to Geant4. Retrieved on September 13, 2020 from <http://geant4-userdoc.web.cern.ch/geant4-userdoc/UsersGuides/IntroductionToGeant4/html/index.html>
- [10] <http://www.sixiangguo.net/code/geant4/AppDevelop/apas06.html>. Accessed 13 September, 2020.
- [11] O. Hernández Rodríguez, M.S. Thesis, University of Texas at El Paso, 2018. Retrieved on September 14, 2020 from <https://scholarworks.utep.edu/dissertations/AAI10823026/>.



Journal of Nuclear Physics, Material Sciences, Radiation and Applications

Chitkara University, Saraswati Kendra, SCO 160-161, Sector 9-C,
Chandigarh, 160009, India

Volume 8, Issue 2

February 2021

ISSN 2321-8649

Copyright: [© 2021 J.A. López et al.] This is an Open Access article published in Journal of Nuclear Physics, Material Sciences, Radiation and Applications (J. Nucl. Phys. Mat. Sci. Rad. A.) by Chitkara University Publications. It is published with a Creative Commons Attribution- CC-BY 4.0 International License. This license permits unrestricted use, distribution, and reproduction in any medium, provided the original author and source are credited.